

DISCRIMINATING WEAK LENSING FROM INTRINSIC SPIN CORRELATIONS USING THE CURL-GRADIENT DECOMPOSITION

ROBERT G. CRITTENDEN¹, PRIYAMVADA NATARAJAN², UE-LI PEN³ & TOM THEUNS⁴

1 Department of Applied Mathematics and Theoretical Physics, Wilberforce Road, Cambridge CB3 0WA, UK

2 Department of Astronomy, Yale University, New Haven, CT 06511, USA

3 CITA, McLennan Labs, University of Toronto, Toronto, M5S 3H8

4 Institute of Astronomy, Madingley Road, Cambridge CB3 0HA, UK

Draft version May 13, 2019

ABSTRACT

The distortion field defined by the ellipticities of galaxy shapes as projected on the sky can be uniquely decomposed into a gradient and a curl component. If the observed ellipticities are induced by weak gravitational lensing, then the distortion field is curl free. Here we show that, in contrast, the distortion field resulting from intrinsic spin alignments is not curl free. This provides a powerful discriminant between lensing and intrinsic contributions to observed ellipticity correlations. We also show how these contributions can be disentangled statistically from the ellipticity correlations or computed locally from circular integrals of the ellipticity field. This allows for an unambiguous detection of intrinsic galaxy alignments in the data. When the distortions are dominated by lensing, as occurs at high redshifts, the decomposition provides a valuable tool for understanding properties of the noise and systematic errors. These techniques can be applied equally well to the polarization of the microwave background, where it can be used to separate curl-free scalar perturbations from those produced by gravity waves or defects.

1. INTRODUCTION

The shapes of distant galaxies can be distorted due to gravitational lensing by the intervening matter distribution (Gunn 1967; see e.g. Bartelmann & Schneider 1999 for a recent review and further references). While the distortions are usually small, a signal can still be detected statistically since neighboring objects will be deformed in a similar way, thereby producing measurable correlations in galaxy shapes. Recently, shape distortions of order 1% have been detected by several groups in deep galaxy surveys on scales from one up to several arc minutes (van Waerbeke et al. 2000, Wittman et al. 2000, Bacon, Refregier & Ellis 2000, Kaiser, Wilson & Luppino 2000). The amplitude of these distortions appears consistent with that predicted from weak lensing by large scale structure.

Weak lensing is not the only possible source of galaxy shape correlations; these can also arise between physically close galaxies as a consequence of the galaxy formation process or subsequent interactions. One possible mechanism for this is the coupling of galaxy spins: galaxy disks tend to be oriented perpendicular to their angular momentum vectors, so angular momentum couplings of neighbors will induce alignments in the projected galaxy shapes. This will also be true but to a lesser extent for elliptical galaxies if they rotate along their shortest axis. The amplitude of the expected shape correlations from angular momentum couplings have recently been studied in numerical simulations by Heavens et al. (2000) and analytically by Crittenden et al. (CNPT 2000), while alternative mechanisms for intrinsic correlations have also been suggested (Croft and Metzler 2000; Catelan et al. 2000). Intrinsic correlations will be especially important in relatively shallow surveys such as the 2dF or the Sloan Digital Sky survey, where the median redshift is $\ll 1$. Evidence for the existence of such intrinsic correlations in the nearby universe has been recently presented by Pen, Lee & Seljak (2000) and Brown et al. (2000), looking in the Tully and the Super COSMOS galaxy catalogs, respectively.

One way of disentangling the intrinsic shape correlations from those induced by weak lensing is to examine the patterns of the average galaxy shapes. The shapes of galaxies are typically described by two degrees of freedom; their average ellipticity and orientation. The distribution of galaxy shapes can be described by a symmetric and traceless 2D tensor field. In general, any such tensor field can be written as a sum of two terms, one of which is curl-free and the other is divergence-free. In analogy with the radiation field in electromagnetism, these are usually referred to as the ‘electric’ (E) and the ‘magnetic’ (B) component, respectively.

Lensing by a point mass will create a tangential, curl-free distortion pattern. The most general distortion field produced by lensing will be a linear superposition of such patterns and will also be a curl-free, (i.e. E -type) field (Kaiser 1992, Stebbins 1996). However, as we show below, the distortion field resulting from intrinsic spin alignments has E and B -type modes of the same order of magnitude. This property will enable us to uniquely disentangle angular momentum correlations and to subtract their contribution from a measured distortion field in order to more accurately compute and isolate the distortions induced by lensing alone. When the deformations are dominated by lensing, the E – B decomposition can improve the signal to noise level, since noise and other systematic effects are expected to contribute to both the E and B channels. Current surveys have measured the sum of E and B powers, thus doubling the noise power relative to the decomposition strategy that we propose here.

The expected amplitude of galaxy shape correlations is fairly small. In order to measure it given the large scatter in the intrinsic shapes of galaxies, many galaxies must be observed. At present, observations of mean ellipticities are dominated by the intrinsic scatter. Direct decomposition into E and B modes is a non-local operation, requiring derivatives of these

noisy observations and so is very problematic. Here we show how the correlation functions of the observable ellipticities can be directly converted into correlations of the E and B -modes.

It is also useful to have locally defined quantities which reflect the E and B decomposition. Kaiser et al. (1994) and Schneider et al. (1998) looked at this issue in the context of lensing and developed a statistic known as the ‘aperture mass’ which enabled them to put a lower bound on the projected mass in a localized region of the sky. More generally, this statistic gives a direct, local measure of the electric contribution to the distortion field, and a similar observable can be evaluated to measure the magnetic component. We develop this formalism here and relate the correlations of these local E and B estimators to those of the observable ellipticities.

This paper is organized as follows. We begin by defining the $E - B$ decomposition in terms of observed ellipticities, and demonstrate that the lensing distortions are curl free, whereas those due to intrinsic alignments are not. In Section 3, we discuss estimators of the $E - B$ correlations and their relation to correlators of the ellipticities. In Section 4, we define the local E and B measures and calculate their correlations. We conclude in sections 5-6 with a cookbook style summary on how the $E - B$ decomposition can be derived from the statistical weak lensing surveys.

2. DECOMPOSITION OF THE DISTORTION FIELD

The projected shape of a galaxy on the sky can be approximated by an ellipse with semi-axes a and b ($a > b$), of which the major axis makes an angle ψ with respect to the x -axis of the chosen coordinate system. It can then be concisely written as a complex number,

$$\epsilon = \frac{(a^2 - b^2)}{(a^2 + b^2)} e^{2i\psi} = \epsilon_+ + i\epsilon_\times, \quad (1)$$

where $\epsilon_+ = |\epsilon| \cos(2\psi)$ and $\epsilon_\times = |\epsilon| \sin(2\psi)$. The phase dependence $\propto e^{2i\psi}$ expresses the fact that the ellipticity is invariant under a rotation over π radians. Note that the two components ϵ_\times and ϵ_+ are analogous to the Q and U Stokes parameters for linearly polarized light. Given a distribution of galaxies on the sky with measured ellipticities, the complex scalar ellipticity field defines a traceless, symmetric 2×2 tensor field,

$$[\gamma]_{ab} = \begin{bmatrix} \epsilon_+ & \epsilon_\times \\ \epsilon_\times & -\epsilon_+ \end{bmatrix}. \quad (2)$$

We have approximated the sky as flat and followed the derivation of Kamionkowski et al. (1998). See Stebbins (1996) for the generalization to a curved sky.

The shear field Eq. (2) can be written in terms of a gradient or ‘ E ’-piece and a curl or pseudo-scalar ‘ B ’-piece (Stebbins 1996) by introducing two scalar functions Φ_E and Φ_B ,

$$\gamma_{ab}(\mathbf{x}) = (\partial_a \partial_b - \frac{1}{2} \delta_{ab} \nabla^2) \Phi_E(\mathbf{x}) + \frac{1}{2} (\epsilon_{cb} \partial_a \partial_c + \epsilon_{ca} \partial_c \partial_b) \Phi_B(\mathbf{x}), \quad (3)$$

where ϵ_{ab} is the anti-symmetric tensor. Each component of the ellipticity field can be written as a function of Φ_E and Φ_B as

$$\begin{aligned} \epsilon_+ &= \gamma_{xx} = -\gamma_{yy} = \frac{1}{2} (\partial_x \partial_x - \partial_y \partial_y) \Phi_E(\mathbf{x}) - \partial_x \partial_y \Phi_B(\mathbf{x}) \\ \epsilon_\times &= \gamma_{yx} = \gamma_{xy} = \partial_x \partial_y \Phi_E(\mathbf{x}) + \frac{1}{2} (\partial_x \partial_x - \partial_y \partial_y) \Phi_B(\mathbf{x}). \end{aligned} \quad (4)$$

The E and B parts can be extracted explicitly from the shear tensor by applying the ∇^4 operator,

$$\nabla^4 \Phi_E = 2 \partial_a \partial_b \gamma_{ab}; \quad \nabla^4 \Phi_B = 2 \epsilon_{ab} \partial_a \partial_c \gamma_{bc}. \quad (5)$$

The relation between the functions Φ_E and Φ_B and the projected gravitational potential will become obvious in what follows. It is useful to perform the $E - B$ decomposition in terms of variables that have the same dimension as the measured ellipticities (Kamionkowski et al. 1998): $\gamma_E \equiv \frac{1}{2} \nabla^2 \Phi_E$ and $\gamma_B \equiv \frac{1}{2} \nabla^2 \Phi_B$. These are related to the ellipticities by

$$\begin{aligned} \nabla^2 \gamma_E &= \partial_a \partial_b \gamma_{ab} = (\partial_x \partial_x - \partial_y \partial_y) \epsilon_+ + 2 \partial_x \partial_y \epsilon_\times \\ \nabla^2 \gamma_B &= \epsilon_{ab} \partial_a \partial_c \gamma_{bc} = (\partial_x \partial_x - \partial_y \partial_y) \epsilon_\times - 2 \partial_x \partial_y \epsilon_+. \end{aligned} \quad (6)$$

Since only the *derivatives* of γ_E and γ_B are defined in terms of the ellipticity field, $\gamma_E(\mathbf{x})$ and $\gamma_B(\mathbf{x})$ are ambiguous up to a constant and linear gradient term. In the same way, constant and linear gradient terms in the measured ellipticities should not impact the $E - B$ decomposition. To see this, consider an ellipticity field where $\epsilon_+(\mathbf{x}) = x$ and $\epsilon_\times(\mathbf{x}) = 0$. This can either be a consequence of a pure E -mode ($\Phi_E = x^3/3$; $\Phi_B = 0$), the result of a pure B -mode ($\Phi_E = 0$; $\Phi_B = x^2 y/2 + y^3/6$), or a linear combination of the two.

A rotation of the basis axes translates ϵ_+ into ϵ_\times and vice versa, but does not affect the $E - B$ decomposition. In particular, the ellipticity measured in a basis which is at an angle φ relative to the original basis is given by:

$$\epsilon'_+ = \epsilon_+ \cos 2\varphi - \epsilon_\times \sin 2\varphi; \quad \epsilon'_\times = \epsilon_+ \sin 2\varphi + \epsilon_\times \cos 2\varphi. \quad (7)$$

Thus, a global rotation of $\pi/4$ transforms $\epsilon'_+ = -\epsilon_\times$; $\epsilon'_\times = \epsilon_+$, but since the position vectors are also rotated, the $E - B$ decomposition remains invariant. However, one can also take an ellipticity field and rotate each ellipticity individually by $\pi/4$, keeping the position vectors fixed. This new ellipticity map has the E and B modes of the original map interchanged: $\gamma'_E = -\gamma_B$; $\gamma'_B = \gamma_E$.

2.1. Distortions due to lensing

In the case of gravitational lensing, the resultant distortion field γ can be written in terms of a gravitational deflection potential ψ as (e.g. Bartelmann and Schneider 1999)

$$\gamma_{ab}(\mathbf{x}) = (\partial_a \partial_b - \frac{1}{2} \delta_{ab} \nabla^2) \psi(\mathbf{x}). \quad (8)$$

The deflection potential ψ is a convolution over the projected surface mass density $\kappa(\mathbf{x})$, $\psi(\mathbf{x}) = \frac{1}{\pi} \int d\mathbf{x}' \kappa(\mathbf{x}') \ln |\mathbf{x} - \mathbf{x}'|$. Comparing this expression to the $E - B$ decomposition of Eq. (3) we can identify $\Phi_E(\mathbf{x}) = \psi(\mathbf{x})$ and $\Phi_B = 0$. Thus for the shear field induced by lensing, the E -mode is related to κ , the projected surface mass density in units of the critical surface mass density for a given configuration of source and lens, and the B -mode is identically zero (as was discussed by Kaiser 1995; Kamionkowski et al. 1998). Note that weak lensing only approximately gives pure E -modes, as B -modes may arise when the light is bent in more than one scattering event. However, these B -modes arise at higher order and are suppressed relative to the E -modes.

If one measures the E -mode contribution of a given map and then rotates every measured ellipticity by $\pi/4$ and repeats the same measurement, one obtains an estimate of the B -contribution which should be consistent with zero for a pure lensing signal. Therefore, the absence of B -modes naturally provides a robust test for isolating the lensing component of the distortion field and provides an estimate of the noise level of the data (Kaiser 1992).

Note that lensing is not the only possible source of curl-free correlations. If the shapes of galaxies are primarily determined by tidal stretching, this would lead to intrinsic correlations (Catelan, Kamionkowski & Blandford, 2000; Croft & Metzler, 2000). For these shape distortions, the observed ellipticities are also linear in the tidal field, leading to pure electric modes just as in lensing. For spiral galaxies which have had many dynamical times to evolve, tidal stretching is likely to be small compared to the contribution from spin alignments. Even for elliptical galaxies, a bulk rotation of as small as 1 km/sec would erase the galaxy's original alignment. Almost all observed ellipticals rotate faster than that, so the shape-shear alignment in Catelan et al. (2000) is unlikely to be observable. However, it could be significant for larger objects like clusters which are dynamically much younger.

2.2. Distortions due to angular momenta alignments

Shape correlations between galaxies can also arise from alignments in the direction of their angular momenta. While this is particularly true for spiral galaxies, given the assumption that their disks are perpendicular to the angular momentum vectors, it is true to a lesser extent for elliptical galaxies as well. Ellipticals probably rotate about their intermediate axis (Dubinski 1992), so averaging over all statistical randomized alignments, the average major axis is perpendicular to the angular momentum vector, just like a spiral galaxy. The strength of the correlation signal has recently been studied in numerical simulations by Heavens et al. (2000). We have recently attempted to model these theoretically (CNPT 2000) by assuming angular momentum is induced by tidal torques. Following the formalism developed by Catelan and Theuns (1996), the correlations can be calculated for Gaussian initial fluctuations using linear theory coupled with the Zeldovich approximation.

The induced intrinsic correlations of ellipticities will primarily result from correlations in the direction of the angular momenta. As discussed in CNPT this implies that the ellipticities are effectively quadratic in the angular momenta,

$$\bar{\epsilon}_+ \propto \frac{1}{2} (\hat{T}_{xi} \hat{T}_{ix} - \hat{T}_{yi} \hat{T}_{iy}); \quad \bar{\epsilon}_\times \propto \frac{1}{2} \hat{T}_{xi} \hat{T}_{iy}. \quad (9)$$

Here, $T_{ij} \propto \partial_i \partial_j \phi$ is the shear of the gravitational potential, and \hat{T} denotes the shear tensor normalized by $\sqrt{T_{ij} T_{ij}}$. Note that i and j run over three coordinates, x, y, z in contrast to above where two dimensional (projected) quantities were considered. The quadratic dependence on the shear in Eq. (9) is fundamentally different from the linear one appropriate for the lensing case, Eq. (8), and as a result the B -modes are non-zero.

In particular, it is straight forward to show that

$$\nabla^2 \gamma_E \propto \hat{T}_{xi,xx} \hat{T}_{ix} + \hat{T}_{yi,yy} \hat{T}_{iy} + \hat{T}_{xi,xy} \hat{T}_{iy} + \hat{T}_{yi,xy} \hat{T}_{ix} + (\hat{T}_{xi,x} + \hat{T}_{yi,y})^2. \quad (10)$$

and similarly

$$\nabla^2 \gamma_B \propto \hat{T}_{xi,xx} \hat{T}_{iy} - \hat{T}_{yi,yy} \hat{T}_{ix} - \hat{T}_{xi,xy} \hat{T}_{ix} + \hat{T}_{yi,xy} \hat{T}_{iy}. \quad (11)$$

The amplitude of the B -modes is comparable to that of the E -modes, as is shown in Figure 1. The presence of B -modes provides a mechanism for disentangling the correlations which arise from lensing from those resulting from intrinsic alignments due to angular momentum couplings.

This is not the sole means of disentangling intrinsic correlations from weak lensing. The observed ellipticity correlations from intrinsic alignments are strongest at low redshifts, while the lensing signal is larger when the sources are at higher redshifts. In addition, morphology distinctions will be useful, since intrinsic correlations of elliptical galaxies are smaller than those of spirals because they are intrinsically more round. Further possible methods for distinguishing lensing from intrinsic correlations are discussed in Catelan, Kamionkowski and Blandford (2000) and CNPT (2000).

3. CORRELATION ESTIMATORS

The decomposition into curl and gradient contributions is most straight forwardly performed in Fourier space (Kamionkowski et al. 1998). However, often it is useful to consider this in real space, as many issues which might complicate

matters in Fourier space, such as finite field size or patchy sampling, are more easily handled in real space. In this section we deal with performing the decomposition statistically in real space using the ellipticity two point functions. This approach is particularly relevant when the observations are noise dominated, such as is the case when there are relatively few galaxies with which to measure the mean ellipticity, which is the case for the current surveys on small scales where most of the lensing signal lies. In the next section, we will address the issue of a local decomposition.

3.1. Correlations in γ_E and γ_B

Here we will relate the correlations of the electric and magnetic shear directly to correlations of the ellipticity. The real space correlation function of γ_E is related to correlation of its corresponding potential, Φ_E , by

$$\xi_E \equiv \langle \gamma_E(\mathbf{x}) \gamma_E(\mathbf{x} + \mathbf{r}) \rangle = \frac{1}{4} \langle \nabla^2 \Phi_E(\mathbf{x}) \nabla^2 \Phi_E(\mathbf{x} + \mathbf{r}) \rangle = \frac{1}{4} \nabla^4 \Xi_E(r), \quad (12)$$

where $\Xi_E(r) \equiv \langle \Phi_E(\mathbf{x}) \Phi_E(\mathbf{x} + \mathbf{r}) \rangle$. An analogous relation holds for γ_B correlations, while the cross correlation, $\langle \gamma_E \gamma_B \rangle$, is zero if the field is invariant under parity transformations.

These correlations can be directly computed from the observed correlations in ϵ_+ and ϵ_\times , defined through

$$C_1(r, \varphi) \equiv \langle \epsilon_+(\mathbf{x}) \epsilon_+(\mathbf{x} + \mathbf{r}) \rangle; \quad C_2(r, \varphi) \equiv \langle \epsilon_\times(\mathbf{x}) \epsilon_\times(\mathbf{x} + \mathbf{r}) \rangle \quad (13)$$

where the ensemble average is over pairs with separation r , for which the separation vector \mathbf{r} makes an angle φ with respect to the chosen basis. The sum of these correlations is rotationally invariant, but their difference depends explicitly on the choice of orientation of the coordinate axes (Kamionkowski et al. 1998).

The required relation between the observed correlations C_1 and C_2 , and the $E - B$ -correlations ξ_E and ξ_B follows from their definitions using Eq. (4) written in terms of derivatives with respect to the separation r :

$$\begin{aligned} C_1(r, \varphi) &= \frac{1}{8} \nabla^4 [\Xi_E(r) + \Xi_B(r)] + \frac{1}{8} \chi [\Xi_E(r) - \Xi_B(r)] \cos 4\varphi \\ C_2(r, \varphi) &= \frac{1}{8} \nabla^4 [\Xi_E(r) + \Xi_B(r)] - \frac{1}{8} \chi [\Xi_E(r) - \Xi_B(r)] \cos 4\varphi, \end{aligned} \quad (14)$$

where $\nabla^4 = 8D^2 + 8r^2 D^3 + r^4 D^4$, the operator $\chi = r^4 D^4$ and $D \equiv \frac{1}{r} \frac{\partial}{\partial r}$. We wish to invert these equations to find expressions for ξ_E and ξ_B in terms of the observable correlation functions.

This inversion can be done most easily in terms of basis independent correlation functions which we shall denote ξ_+ and ξ_\times . Physically, ξ_+ corresponds to the correlation function $\langle \epsilon_+(\mathbf{x}) \epsilon_+(\mathbf{x} + \mathbf{r}) \rangle$ computed in such a way that, for each pair of galaxies, one coordinate axis is always taken parallel to the separation vector \mathbf{r} . A similar definition holds for ξ_\times in terms of $\langle \epsilon_\times \epsilon_\times \rangle$, while by isotropy, the expectation of the cross correlation is zero. These correlations are related by a rotation to $C_1(r, \varphi)$ and $C_2(r, \varphi)$ and satisfy the relations,

$$\xi_+(r) + \xi_\times(r) = C_1(r, \varphi) + C_2(r, \varphi); \quad [\xi_+(r) - \xi_\times(r)] \cos(4\varphi) = C_1(r, \varphi) - C_2(r, \varphi). \quad (15)$$

In terms of these new observables, Eq. (14) simplifies to

$$4[\xi_+(r) + \xi_\times(r)] = \nabla^4 [\Xi_E(r) + \Xi_B(r)]; \quad 4[\xi_+(r) - \xi_\times(r)] = \chi [\Xi_E(r) - \Xi_B(r)]. \quad (16)$$

Initial measurements of the lensing signal have focused primarily on the variance of the magnitude of the ellipticity averaged over regions of a given size, and its fall off as the size of the regions is increased. The variance is simply the value of the correlation $C_1 + C_2$, convolved with the appropriate window function, at zero lag. The variance has the advantage that it is a local quantity and is straight forward to measure. However, the measurements of the variance at different scales have strongly correlated errors. In addition, since $C_1 + C_2 = \frac{1}{8} \nabla^4 (\Xi_E + \Xi_B)$, such measurements are unable to distinguish E -modes from B -modes. Therefore, it is advantageous to investigate the full correlation functions.

The inversion of Eq. (14) can now be written as,

$$\begin{aligned} \xi_E(r) &= \frac{1}{2} [\xi_+(r) + \xi_\times(r)] + \frac{1}{2} \nabla^4 \chi^{-1} [\xi_+(r) - \xi_\times(r)] \\ \xi_B(r) &= \frac{1}{2} [\xi_+(r) + \xi_\times(r)] - \frac{1}{2} \nabla^4 \chi^{-1} [\xi_+(r) - \xi_\times(r)]. \end{aligned} \quad (17)$$

An equivalent set of equations follows by applying $\chi \nabla^{-4}$ operator to both sides of these equations.

$$\begin{aligned} \chi \nabla^{-4} \xi_E(r) &= \frac{1}{2} \chi \nabla^{-4} [\xi_+(r) + \xi_\times(r)] + \frac{1}{2} [\xi_+(r) - \xi_\times(r)] \\ \chi \nabla^{-4} \xi_B(r) &= \frac{1}{2} \chi \nabla^{-4} [\xi_+(r) + \xi_\times(r)] - \frac{1}{2} [\xi_+(r) - \xi_\times(r)]. \end{aligned} \quad (18)$$

This form actually proves more useful in practice since, as we show below, $\chi \nabla^{-4}$ is more local than $\nabla^4 \chi^{-1}$. Note that these expressions assume statistical isotropy, that is, $\langle \epsilon_+ \epsilon_\times \rangle = 0$ in the basis where the axes are aligned with the galaxy separation vector.

3.2. Evaluation of $\nabla^4 \chi^{-1}$ and $\chi \nabla^{-4}$

It is quite useful to take these relationships into Fourier space, and the operators ∇^4 and χ have particularly simple expressions when applied to the Bessel functions which arise in a Fourier transform. In particular,

$$\nabla^4 J_0(kr) = k^4 J_0(kr); \quad \chi J_0(kr) = k^4 J_4(kr). \quad (19)$$

When combined with the above equations, we can relate the correlation functions directly to the E and B power spectra, reproducing the relations Eqs. (14) and (15) of Kamionkowski et al. (1998). Also, it is straightforward to show that since the power spectrum is the Fourier transform of the correlation function, $\xi_E(r) = \int kdk J_0(kr) P_E(k)$ implies that $\chi \nabla^{-4} \xi_E(r) = \int kdk J_4(kr) P_E(k)$.

The operators $\nabla^4 \chi^{-1}$ and $\chi \nabla^{-4}$ are also most easily evaluated in Fourier space and can be shown to take the form,

$$\begin{aligned} \nabla^4 \chi^{-1} g(r) &= \int \frac{kdk}{2\pi} J_0(kr) \int r' dr' J_4(kr') g(r') = \int r' dr' g(r') \mathcal{G}(r, r') \\ \chi \nabla^{-4} g(r) &= \int \frac{kdk}{2\pi} J_4(kr) \int r' dr' J_0(kr') g(r') = \int r' dr' g(r') \mathcal{G}(r', r), \end{aligned} \quad (20)$$

where

$$\mathcal{G}(r', r) = \int \frac{kdk}{2\pi} J_0(kr) J_4(kr'). \quad (21)$$

Note that since the k integral is from zero to infinity, $rr' \mathcal{G}(r, r')$ depends only on the ratio r/r' . This operator is not simply a convolution as would be the case if $\mathcal{G}(r, r')$ were a function only of the difference $|\mathbf{r} - \mathbf{r}'|$. In fact, the Fourier space operator takes nearly the same form as the real space operator. That is, if the Fourier transform of $g(r)$ is $g(k)$, then the transform of $\int r' dr' g(r') \mathcal{G}(r, r')$ is $\int k' dk' g(k') \mathcal{G}(k', k)$.

Alternatively, these operators can be written in integral form,

$$\begin{aligned} \nabla^4 \chi^{-1} g(r) &= g(r) + 4 \int_r^\infty dr' \frac{g(r')}{r'} - 12r^2 \int_r^\infty dr' \frac{g(r')}{r'^3} \\ \chi \nabla^{-4} g(r) &= g(r) + \frac{4}{r^2} \int_0^r dr' g(r') r' - \frac{12}{r^4} \int_0^r dr' g(r') r'^3. \end{aligned} \quad (22)$$

The second form is the more useful in practice, being more local. To evaluate it at some radius R , one only needs to know the form of $g(r)$ for $r < R$, whereas the $\nabla^4 \chi^{-1}$ requires knowing $g(r)$ for $r > R$.

The particular form of the first of the integral operators follows from choosing integration constants such that $\nabla^4 (\Xi_E(r) + \Xi_B(r))$ does not diverge at large separations. To obtain the second form, we demand that $\chi(\Xi_E(r) - \Xi_B(r))$ and its derivatives are well-behaved as $r \rightarrow 0$. The origin of these integration constants is the constant and linear gradient ambiguities in the definitions of γ_E and γ_B in Section 2.

3.3. Power law solutions

As an illustration, consider the case where the correlation functions both behave as power laws with the same index, $\xi_+(r) = Ar^n$ and $\xi_-(r) = Br^n$. Note that $\nabla^4 \chi^{-1} r^n = f(n)r^n$, where $f(n) = (n^2 + 6n + 8)/(n^2 - 2n)$. It then follows that

$$\xi_{E,B} = f(n) \chi \nabla^{-4} \xi_{E,B} = \frac{1}{2} [(A + B) \pm (A - B)f(n)] r^n. \quad (23)$$

Note that for certain power laws, $n = -2$ or $n = -4$, the operator $\nabla^4 \chi^{-1} r^n = 0$, while it diverges when $n = 0$ or $n = 2$. The opposite is true for the inverse operator $\chi \nabla^{-4}$, which diverges when $n = -2$ or $n = -4$ and is zero for $n = 0$ or $n = 2$.

In the case when the B -modes are exactly zero, as occurs for gravitational lensing, one obtains $(A + B) = (A - B)f(n)$. It follows that the ratio of the correlation functions is given by

$$\xi_+/\xi_- = \frac{n^2 + 2n + 4}{4(n + 1)}. \quad (24)$$

This expression diverges when $n = -1$ which therefore implies that $\xi_- = 0$ in this case. Kaiser (1992) also considered power law spectra in the lensing case and presented results for a number of spectral indices. Our results agree qualitatively, but the agreement is not exact. Kaiser calculated these numerically and this may be the source of the discrepancies.

3.4. Application to spin correlations

We can apply this technique to the correlations arising from intrinsic spin couplings. The ellipticity correlations were calculated for the model described in CNPT (2000), and we will not go into further detail here. Using the CNPT results and the above expressions, we can calculate the E and B correlation functions and these are presented in Figure 1. In contrast to the gravitational lensing cases, the E and B modes are seen to be of comparable magnitude in this model.

Various parameter choices have been made in the examples we have shown, but we believe the $E - B$ decomposition to be largely independent of most of these. For simplicity, the figures assume the galaxies are effectively perfect disks ($a = 1$ in the notation of CNPT). Using more realistic galaxy shapes will only suppress the overall amplitude of the correlations. We

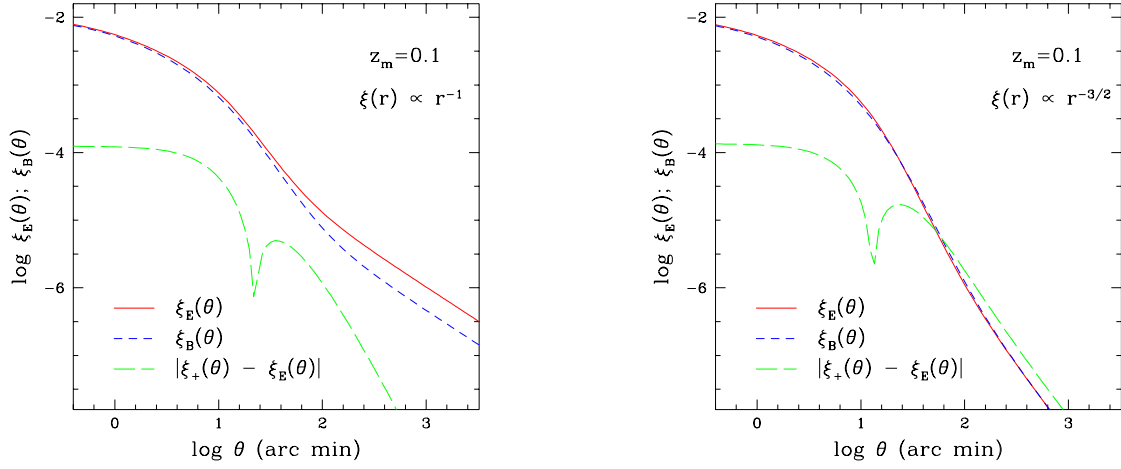


FIG. 1.— The E and B -mode correlation functions for intrinsic spin correlations in the model of CNPT (2000). The amplitude of the correlations are determined by the parameters a and α , which have been taken to be unity for simplicity. The mean redshift of the sources was taken to be $z_m = 0.1$ and the density correlations were taken to fall off as r^{-1} in the left figure and as $r^{-3/2}$ in the right figure. Also plotted are the differences between ξ_E and ξ_+ , which is the same as the differences between ξ_B and ξ_\times . In the left panel, the projected ellipticity correlations fall off as θ^{-1} and ξ_E and ξ_+ are very nearly the same. This is not the case in general, as can be seen in the right panel where the projected correlations fall as θ^{-2} . However, the θ^{-2} is also special in that ξ_E and ξ_B are nearly identical.

have also assumed that the angular momentum directions correspond with those that would be predicted by linear theory ($\alpha = 1$.) Non-linear evolution may affect the direction of a galaxy's angular momentum, but as long as these changes are not coherent then they will only suppress the overall correlation amplitudes. Finally, we have assumed a mean redshift for the sources of $z_m = 0.1$. Changing this will change the angular scale at which a given level of correlations are seen, but it should not affect the nature of the $E - B$ decomposition.

As discussed above, one factor which could affect the $E - B$ decomposition is the rate at which ellipticity correlations drop off. The case when the density correlation falls off as r^{-1} implies that for large separations, the projected ellipticities fall off as θ^{-1} , where θ is the angular separation. Since $f(-1) = 1$, ξ_E will be the same as ξ_+ , and ξ_B will be the same as ξ_\times . This is shown in the left panel of Figure 1. Also shown in the right panel is the case when the density correlation falls off as $r^{-3/2}$ and the projected ellipticity drops as θ^{-2} . In this case, $f(-2) = 0$ and $\xi_E = \xi_B = \frac{1}{2}(\xi_+ + \xi_\times)$. Note that here the \times modes are actually anti-correlated at large separations.

4. LOCAL CORRELATORS

Here we will consider local estimators of the E and B modes. These are generalizations of the 'mass aperture' formalism of the pure lensing case, proposed by Kaiser et al. (1994) and developed further by Schneider et al. (1998) and applied to CMB polarization by Seljak and Zaldarriaga (1998). They showed that a convolution of the tangential shear with a given wavelet provided a measure of the projected mass convolved with a related wavelet. More generally, the integrals of the tangential shape distortions can be directly related to the local 'electric' distortion. Thus E -modes are associated with either tangential or radial patterns, as shown in Figure 2 (left panel.) B -modes are also related to the circular distortion pattern, but these have an associated 'handedness' or orientation, as shown in the right panel of Figure 2.

The local correlators are most easily defined by considering polar coordinates about a given point. The E -mode is related to the tangential shear, which is the local ϵ_+ (or Q Stokes parameter) in a coordinate system defined by the radial vector to that point. The B -mode corresponds analogously with the local ϵ_\times mode (or U Stokes parameter) in the same basis and can be thought of as a $\pi/4$ shear. These quantities are related to the original ellipticity field by a φ dependent rotation:

$$\gamma_t = \epsilon_+ \cos(2\varphi) + \epsilon_\times \sin(2\varphi); \quad \gamma_{\frac{\pi}{4}} = \epsilon_\times \cos(2\varphi) - \epsilon_+ \sin(2\varphi). \quad (25)$$

Figure 2 shows modes where $\gamma_t(\varphi)$ and $\gamma_{\frac{\pi}{4}}(\varphi)$ are independent of φ .

It is possible to show that circular integrals of γ_t and $\gamma_{\frac{\pi}{4}}$ are directly related to the γ_E and γ_B contained interior to the circle. Using the relations of Eq. (4) in polar coordinates, one can show

$$\gamma_t = \frac{1}{2} \left(\frac{\partial^2}{\partial r^2} - \frac{1}{r} \frac{\partial}{\partial r} - \frac{1}{r^2} \frac{\partial^2}{\partial \varphi^2} \right) \Phi_E - \left(\frac{\partial}{\partial r} \frac{1}{r} \frac{\partial}{\partial \varphi} \right) \Phi_B; \quad \gamma_{\frac{\pi}{4}} = \frac{1}{2} \left(\frac{\partial^2}{\partial r^2} - \frac{1}{r} \frac{\partial}{\partial r} - \frac{1}{r^2} \frac{\partial^2}{\partial \varphi^2} \right) \Phi_B + \left(\frac{\partial}{\partial r} \frac{1}{r} \frac{\partial}{\partial \varphi} \right) \Phi_E. \quad (26)$$

We can use the polar form of ∇^2 to relate the derivatives of the potential to γ_E . If we integrate these equations over φ ,

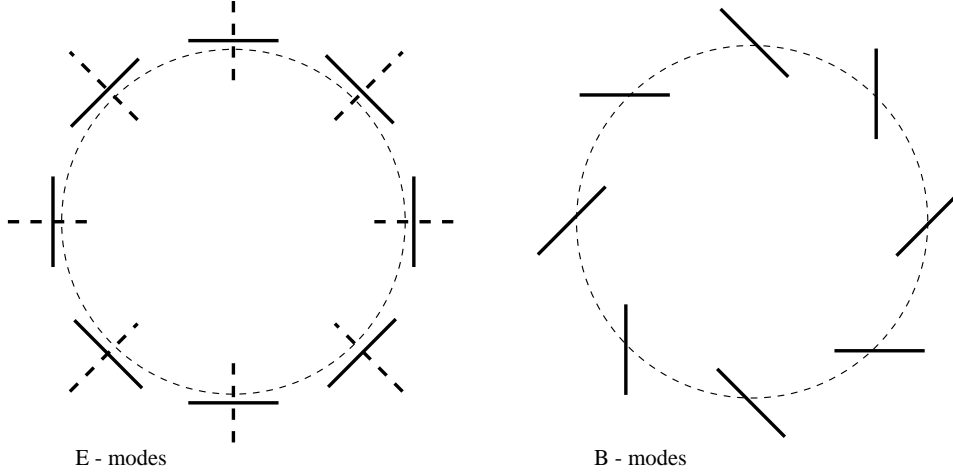


FIG. 2.— Local representations of E (gradient) and B (curl) modes. E -modes are either tangential or radial, depending on their sign. B -modes can be oriented in either a clockwise or counter-clockwise (shown) direction. Lensing generally brings about only E -modes, while noise and angular momentum correlations can generate both. Local estimators of the E and B -modes can be found by doing a radial weighting of these circular integrals (Kaiser et al. 1994).

the derivatives with respect to φ drop out and it can be shown that

$$\begin{aligned} \frac{1}{2\pi} \int_0^{2\pi} d\varphi \gamma_E(\mathbf{r}) &= \frac{1}{2\pi} \int_0^{2\pi} d\varphi \gamma_t(\mathbf{r}) + \frac{1}{\pi r^2} \int_0^r r' dr' \int_0^{2\pi} d\varphi \gamma_E(\mathbf{r}') \\ &= \frac{1}{2\pi} \int_0^{2\pi} d\varphi \gamma_t(\mathbf{r}) + 2 \int_0^r \frac{dr'}{r'} \frac{1}{2\pi} \int_0^{2\pi} d\varphi \gamma_t(\mathbf{r}') \end{aligned} \quad (27)$$

A similar relation holds when replacing $\gamma_E \rightarrow \gamma_B$ and $\gamma_t \rightarrow \gamma_{\frac{\pi}{4}}$.

We can convolve these relations with a compensated filter $\hat{\mathcal{U}}(r)$. This filter may be arbitrary, but we will require that $\int d^2r \hat{\mathcal{U}}(r) = 0$. For example, one might take it to have the shape of a Mexican hat. Multiplying both sides by $r\hat{\mathcal{U}}(r)$ and integrating over r one obtains the local estimators

$$\begin{aligned} \Gamma_E &\equiv \int d^2r \gamma_E(\mathbf{r}) \hat{\mathcal{U}}(r) = \int d^2r \gamma_t(\mathbf{r}) \mathcal{Q}(r) \\ \Gamma_B &\equiv \int d^2r \gamma_B(\mathbf{r}) \hat{\mathcal{U}}(r) = \int d^2r \gamma_{\frac{\pi}{4}}(\mathbf{r}) \mathcal{Q}(r), \end{aligned} \quad (28)$$

where it follows by integrating by parts that $\mathcal{Q}(r) = \hat{\mathcal{U}}(r) - \frac{2}{r^2} \int_0^r r' \hat{\mathcal{U}}(r') dr'$. $\hat{\mathcal{U}}(r)$ can be taken to be zero outside a given radius, so these relations become purely local. Thus we have a local measure of the $E - B$ decomposition related solely to the ellipticity in that region. In the absence of instrumental and sampling noise, lensing predicts that Γ_B will be identically zero for any point on the sky.

The correlations of these local measures can be computed as follows,

$$\begin{aligned} \langle \Gamma_E(0) \Gamma_E(R) \rangle &= \int \frac{d^2k}{2\pi} \hat{\mathcal{U}}^2(k) e^{i\mathbf{k} \cdot \mathbf{R}} \int d^2r \langle \gamma_E(0) \gamma_E(r) \rangle e^{i\mathbf{k} \cdot \mathbf{r}} \\ &= \int d^2r \frac{1}{2} [(\xi_+(r) + \xi_*(r)) + \nabla^4 \chi^{-1} \{ \xi_+(r) - \xi_*(r) \}] \mathcal{W}(|\mathbf{r} + \mathbf{R}|) \\ &= \frac{1}{2} \int d^2r [\xi_+(r) + \xi_*(r)] \mathcal{W}(|\mathbf{r} + \mathbf{R}|) + \frac{1}{2} \int d^2r [\xi_+(r) - \xi_*(r)] \tilde{\mathcal{W}}(|\mathbf{r} + \mathbf{R}|), \end{aligned} \quad (29)$$

where we used Eq. (17), and defined $\hat{\mathcal{W}}(k) \equiv \hat{\mathcal{U}}^2(k)$, so that $\mathcal{W}(r)$ is the convolution of $\hat{\mathcal{U}}(r)$ with itself. The function $\tilde{\mathcal{W}}(r)$ can be shown to be a convolution of $\mathcal{W}(r)$ and $\mathcal{G}(r, r')$, i.e.

$$\int r dr \mathcal{W}(r) \nabla^4 \chi^{-1} g(r) = \int r dr \mathcal{W}(r) \int r' dr' \mathcal{G}(r, r') g(r') = \int r' dr' g(r') \tilde{\mathcal{W}}(r'). \quad (30)$$

From this it follows that $\tilde{\mathcal{W}}(r') \equiv \int r dr \mathcal{W}(r) \mathcal{G}(r, r') = \chi \nabla^{-4} \mathcal{W}(r')$. The corresponding expression for the B -mode is

$$\langle \Gamma_B(0) \Gamma_B(R) \rangle = \frac{1}{2} \int d^2r [\xi_+(r) + \xi_*(r)] \mathcal{W}(|\mathbf{r} + \mathbf{R}|) - \frac{1}{2} \int d^2r [\xi_+(r) - \xi_*(r)] \tilde{\mathcal{W}}(|\mathbf{r} + \mathbf{R}|). \quad (31)$$

The variances of the E or B field smoothed with a given window $\hat{\mathcal{U}}(r)$ is obtained by setting the separation $R = 0$. Note that as in the previous section, we are implicitly incorporating statistical isotropy in these correlation expressions.

For concreteness, it is useful to consider a simple example of a wavelet shape. Following work by van Waerbeke (1998), assume the radial function to have the form of a Mexican hat wavelet, which is the derivative of a Gaussian function,

$\mathcal{U}(r) = \sigma^{-2} (1 - r^2/2\sigma^2) \exp(-r^2/2\sigma^2)$ and its Fourier transform is simply $\hat{\mathcal{U}}(k) = \frac{1}{2}k^2\sigma^2 e^{-k^2\sigma^2/2}$. For this particular choice, the convolution of $\mathcal{U}(r)$ with itself is $\mathcal{W}(r) = (1/2\sigma^2) [2 - r^2/\sigma^2 + r^4/16\sigma^4] \exp(-r^2/4\sigma^2)$. Finally, using the fact that the Fourier representation of ∇^{-4} is k^{-4} , we have,

$$\tilde{\mathcal{W}}(r) = \chi \left[\frac{\sigma^2}{2} e^{-r^2/4\sigma^2} \right] = \frac{1}{2\sigma^2} \left(\frac{r^2}{4\sigma^2} \right)^2 e^{-r^2/4\sigma^2}. \quad (32)$$

This particular wavelet has the advantages that it is simple, analytic and very compact, falling off exponentially at large distances.

5. DATA ANALYSIS

In this section we address the direct analysis of real survey data. We first consider the extraction of the E and B correlators. For this purpose, one only needs to measure the two pairwise ellipticity correlation functions ξ_+, ξ_\times (defined before Eqn (15)) for all pairs of galaxies as a function of separation, which has been done by van Waerbeke et al, (2000) and does not depend on the geometry of the survey or its boundary shapes. This correlation function (plus its error bars and the covariance matrix of errors) contains all the second order statistics of the map, and is a complete and optimal two point description.

We now have two functions, both of which contain noise, and our goal is to apply a rotation such that one function contains lensing signal and the other no lensing signal, but which will give an estimate of contamination from noise and intrinsic correlations. The current analyses effective have added the two correlations, which adds a function which contains lensing to one which contains no lensing but an equal amount of noise, which doubles the amount of noise we have. Instead, we can define $\xi'(r) = 2/r^2 \int_0^r [\xi_+(r') + \xi_\times(r')] r' dr' - 6/r^4 \int_0^r [\xi_+(r') + \xi_\times(r')] r'^3 dr'$. We can now derive pure E -type and B -type correlators which depend only on correlations at separations less than r ,

$$\begin{aligned} \chi \nabla^{-4} \xi_E(r) &= \int kdk J_4(kr) P_E(k) = \xi_+(r) + \xi'(r) \\ \chi \nabla^{-4} \xi_B(r) &= \int kdk J_4(kr) P_B(k) = \xi_\times(r) + \xi'(r) \end{aligned} \quad (33)$$

In the case of pure weak lensing, the B -type correlator should be consistent with pure noise, while ξ_E contains all the lensing signal, and only half the noise. We have achieved the correlation function analogy of Kaiser's 45 degree rotation: rotating all the images by 45 degrees swaps ξ_E and ξ_B .

One can also obtain expressions for the variances of the fields smoothed by a tophat filter with radius R . This is done by convolving the correlation functions with a window which is proportional to the area of overlap between two circles of radius R and separation r ,

$$\langle \gamma_E^2(R) \rangle_{TH} = \frac{2}{\pi R^4} \int_0^{2R} r dr \xi_E(r) \left(2R^2 \cos^{-1}(r/2R) - r \sqrt{R^2 - r^2/4} \right). \quad (34)$$

This again contains half as much noise power as the standard procedure of actually convolving the map and computing its variance, which is what all work to date has performed.

This decomposition was performed directly on the correlator, and there exists no transformation on the shear map such that the correlation function of the transformed shear map is given by Eqn. (33). Similarly, Eqn. (34) is not identically equal to the tophat smoothed map variance. If one actually wants to make a map, the aperture shear decomposition Eqn. (28) allows one to make a local decomposed map, whose variance one can then measure. Note that in making a map, one loses information near the boundaries, and variation in source counts leads to inhomogeneous signal-to-noise, decreasing the overall sensitivity to measuring the true correlation function. Luckily the aperture mass approach also allows a direct computation of the same quantities from the correlation functions, as shown in Eqn. (31).

6. CONCLUSIONS

Here we have investigated the general decomposition of flat two dimensional spin-2 fields into so-called electric (gradient) and magnetic (curl) components. While this decomposition involves derivatives and is intrinsically non-local, we have shown how local correlations of the electric and magnetic components can be found given correlations in the components of the ellipticity (Equations 17 and 18). For the case of power law correlations, this implies a relationship between the spectral index of the correlations and the relative amplitude of the different types of ellipticity correlations.

In addition, following Kaiser et al. (1994) we have shown how local estimators for the electric and magnetic modes can be constructed from circular integrals of the tangential and $\pi/4$ (or Q and U Stokes parameters) distortions respectively (Figure 2). We calculated correlations of these local estimators and related them to the ellipticity correlations.

This decomposition has important consequences when applied to the projected shapes of galaxies. Gravitational lensing primarily produces electric modes, as does the tidal stretching of galaxies. However, as we have shown here, angular momentum couplings produce E and B -modes in comparable amounts and one might expect that noise, telescope distortions and other sources of systematic errors will produce curl modes as well.

Thus the presence of B -modes will be useful for disentangling intrinsic correlations caused by angular momentum couplings from those induced by cosmic shear and from gravitational lensing. Even if lensing distortions dominate, this decomposition will be useful as a means of estimating the levels of noise and systematic errors in the observations. In addition, it provides a means of reducing noise levels of lensing observations by a factor of $\sqrt{2}$ (Kaiser 1995.)

The prospects for isolating the contribution of B -modes using these local correlators are promising with several of the ongoing shallow redshift and imaging surveys presently taking data. These include the Sloan DSS (www.sdss.org), 2dF (www.ast.cam.ac.uk/AAO/2df), 2MASS (pegasus.phast.umass.edu), DEEP (dls.bell-labs.com) and the INT wide field survey (www.ast.cam.ac.uk/~wfcsur/). The low median redshift implies minimal contamination from the lensing signal and therefore an improvement in the signal to noise of the extraction.

Finally, most of these considerations apply equally well to the imminent observations of CMB polarization (e.g. Kamionkowski, Kosowsky & Stebbins 1997; Zaldarriaga & Seljak 1997). In this case, scalar fluctuations induce only E -modes, while noise and gravitational radiation induce both E and B -modes. As in the case of galaxy shapes, these observations will be initially noise dominated, so these kinds of correlation analyses will be essential. The lessons we learn from the lensing data now available will be directly applicable to the polarization data when they become available in a few years time.

We thank Ben Metcalf, Neil Turok and Ludo van Waerbeke for useful conversations. RC and TT acknowledge PPARC for the award of an Advanced and a post-doctoral fellowship, respectively.

REFERENCES

Bacon,D., Refregier, A., Ellis, R., 2000, MNRAS in press astro-ph/0003008

Bartelmann, M., Schneider, P., 1999, preprint, astro-ph/9912508

Brown M.L., Taylor, A.N., Hambly, N.C., Dye, S., 2000, preprint, astro-ph/0009499

Catelan, P., Theuns, T., 1996, MNRAS, 282, 436

Crittenden, R., Natarajan, P., Pen, U., & Theuns, T., 2000, submitted to ApJ (astro-ph/0009052) [CNPT]

Dubinski, J. 1992, ApJ, 401, 441

Gunn, J.E., 1967, ApJ, 150, 737

Kaiser, N., 1992, ApJ, 388, 272

Kaiser, N., 1995, ApJ, 439, L1

Kaiser, N., Squires, G., Fahlman, G., Woods, D., 1994, in Durrett F., Maxure A., Tran Thanh Van J., eds, Clusters of Galaxies, Editions Frontières, Gif-sur-Yvette, p.269

Kaiser, N., Wilson, G., Luppino, G.A., 2000, preprint, astro-ph/0003338

Kamionkowski, M., Kosowsky & Stebbins, A., 1997, Phys.Rev. D55 7368-7388

Kamionkowski, M., Babul, A., Cress, C. M., & Refregier, A., 1998, MNRAS, 301, 1064

Lee, J., & Pen, U., 2000, ApJ, 532, L5 [LP00]

Lee, J., & Pen, U., 2000, astro-ph/0008135

Pen, U., 2000, ApJ, 534, L19.

Pen, U., Lee, J., & Seljak, U., 2000, ApJ 543, L107.

Schneider, P., van Waerbeke, L., Jain, B., Kruse, G., 1998, MNRAS, 296, 873

Seljak, U. & Zaldarriaga, M., 1998, to appear in "Fundamental Parameters in Cosmology," proceedings of the XXXIIIrd Rencontres de Moriond.

Stebbins, A. 1996, astro-ph/9609149

van Waerbeke, L., Bernardeau, F., Mellier, Y., 1999, A&A, 342, 14

van Waerbeke, L., 1998, A&A, 334, 1

Wittman, D. M., Tyson, J. A., Kirkman, D., Dell'Antonio, I. and Bernstein, G. 2000, Nature, 405, 143

Zaldarriaga, M. & Seljak, U., 1997, Phys.Rev. D55, 1830-1840